EUROPHYSICS LETTERS 15 February 2001

Europhys. Lett., **53** (4), pp. 451–457 (2001)

Globally coupled logistic maps as dynamical glasses

S. C. Manrubia[1,2] and A. S. Mikhailov[1]

[1] *Fritz-Haber-Institut der Max-Planck-Gesellschaft*
Faradayweg 4-6, 14195 Berlin, Germany
[2] *MPI for Colloids and Interfaces, Theory Division*
14424 Potsdam, Germany

(received 21 July 2000; accepted in final form 29 November 2000)

PACS. 05.45.-a – Nonlinear dynamics and nonlinear dynamical systems.
PACS. 05.45.Xt – Synchronization; coupled oscillators.
PACS. 75.10.Nr – Spin-glass and other random models.

Abstract. – We compute distributions of overlaps between replicas and discuss replica symmetry breaking in a large dynamical system formed by globally coupled logistic maps under partial synchronization conditions. By computing and analyzing three-replica overlap distributions, the ultrametric hierarchical organization of attractors in this system is tested.

Numerical simulations of various dynamical systems, such as arrays of locally coupled chaotic maps [1], the complex Ginzburg-Landau equation [2], and ensembles of phase oscillators with frustrated interactions [3], show complex collective behaviour resembling that of a spin glass. Globally coupled logistic maps (GCLM) represent the most extensively investigated example of a system with such glass-like behaviour. As shown by Kaneko [4, 5], in the regime of dynamical clustering GCLM are characterized by the coexistence of many different dynamical attractors with fractal attraction basins. It has been found [6] that inside the parameter region of clustering the temporal averages do not coincide in the long-time limit with the ensemble averages and therefore the dynamics of GCLM is non-ergodic (see also [5]).

The theoretical description and analysis of equilibrium spin glasses are based on the notion of replicas and the concept of replica-symmetry breaking [7]. This property has been proven for the mean-field Sherrington-Kirkpatrick (SK) model [8, 9], and confirmed by numerical studies [10, 11] of this and other models of equilibrium spin glasses. Such behaviour was also found in equilibrium physical systems in the absence of quenched disorder [12]. A related concept is that of ultrametric hierarchical organization of replicas [13]. The ultrametricity has been analytically [8] and numerically [14] shown for the SK model.

Though replicas were originally introduced as formal mathematical constructions, they can be interpreted as corresponding to different statistical realizations of the same equilibrium system [9], allowing to extend the concept of replica to systems far from thermal equilibrium. Recently, the glass-like kinetic properties of folding proteins were discussed and different dynamical trajectories of the same system were viewed as its various replicas [15] (see also the model [3] of coupled oscillators and its analysis [16]).

In this letter we introduce an analogous replica description for globally coupled logistic maps. The distributions of overlaps for this system are numerically determined in two different parameter regions, where "glassy" behaviour was previously reported by Kaneko [4] and Vulpiani *et al.* [6]. Three-replica overlap distributions are also computed and investigated to

test the ultrametric properties of GCLM in these parameter regions. The obtained data is used to discuss differences and similarities between GCLM and equilibrium glasses.

The system of globally coupled logistic maps is described by the set of equations [4]

$$x_i(t+1) = (1-\epsilon)f(x_i(t)) + \frac{\epsilon}{N}\sum_{j=1}^{N} f(x_j(t)) \ , \tag{1}$$

where $f(x) = 1 - ax^2$, the parameter ϵ specifies the coupling strength, $i = 1, 2, ..., N$ and N is the system size. The control parameter a of a logistic map shall be chosen in such a way that the dynamics of an individual map is chaotic. When ϵ is sufficiently high, the motion of all maps becomes synchronous while remaining chaotic. The transition to full chaotic synchronization is preceded by a broad interval of coupling strengths where dynamical clustering is observed [4]. In this interval, the system builds a number of coherent clusters. Depending on the initial condition, the system can evolve to different cluster partitions at the same parameter values. A partition is specified by the total number $\mathcal{K}$ of clusters and the numbers N_k of elements in each of them ($k = 1, \ldots, \mathcal{K}$). The partitions differ not only in the number of clusters, but also in their relative sizes. Every cluster partition (each corresponding to an attractor of this system) has its own dynamics, which may be chaotic, quasiperiodic or periodic.

Starting from a random initial condition, in numerical simulations we let the system (1) evolve until it reaches the final attractor. The transient time t_0 depends strongly on the parameters ϵ and a and varies between 10^2 and 10^6 [17, 18]. In all our simulations, we have checked that the attractor at time $t = t_0$ was the same present at time $t' = 2t_0$. Once the dynamical stationary situation is reached, we compute the clustering properties of this final state, *i.e.* determine the elements N_k belonging to each of the clusters $k = 1, \ldots, \mathcal{K}$. We use an exact clustering condition, *i.e.* two elements belong to the same cluster if they have exactly the same states down to the double computer precision. To avoid degeneracy due to the original arbitrary labelling of elements, we reorder them by assigning labels x_1 to x_{N_1} to those in the largest cluster, x_{N_1+1} to x_{N_2} to maps in the second largest cluster, and so on.

Replicas represent dynamic realizations of this system corresponding to different initial conditions. Thus, a replica is a certain orbit $\{x_i(t)\}$ of the entire ensemble. To compare replicas, it is convenient to transform them to binary sequences. At any discrete time t for any element i we assign a binary number $\sigma_i(t)$, such that $\sigma_i(t) = 1$, if $x_i(t) \geq x^*$ and $\sigma_i(t) = -1$, if $x_i(t) < x^*$, where $x^* = (1/2a)\left(-1 + \sqrt{1+4a}\right)$ is the fixed point of a single logistic map. Hence, any replica α is encoded as a certain "spin-chain" configuration $\{\sigma_i^{(\alpha)}(t)\}$. The overlap $q^{\alpha\beta}$ between two replicas α and β, yielded by two different randomly chosen sets of initial conditions $\boldsymbol{x}^{(\alpha)}(0)$ and $\boldsymbol{x}^{(\beta)}(0)$ for the same parameters a and ϵ, can then be computed as

$$q^{\alpha\beta} = \frac{1}{NT}\sum_{t=t_0}^{t_0+T}\sum_{i=1}^{N}\sigma_i^{(\alpha)}(t)\sigma_i^{(\beta)}(t) \ . \tag{2}$$

The time t_0 is chosen large enough to assure that the transient is discarded.

Two periodic orbits can be identical up to a certain time lag (*i.e.* a phase shift). If we directly apply definition (2), different overlaps depending on the phase shift will be in this case detected. To eliminate this effect, we always additionally maximize $q^{\alpha\beta}$ with respect to possible phase shifts [19]. In the cases here investigated, it was enough to consider phase shifts in the range from 2 to 32, since higher periods were practically absent. For chaotic trajectories such optimization is not actually needed if T is long enough. Using the above definition, we

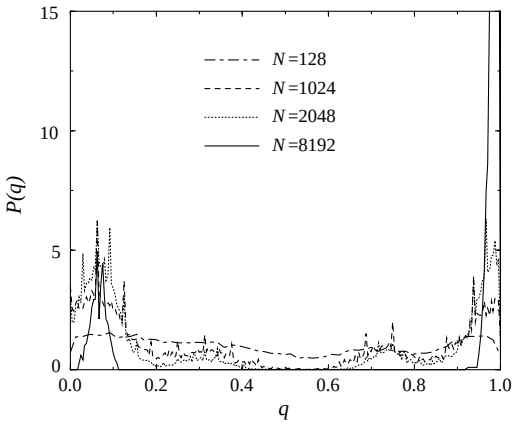

Fig. 1

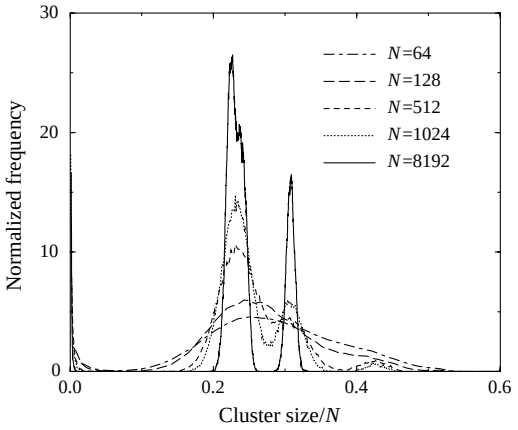

Fig. 2

Fig. 1 – Normalized overlap distributions $P(q)$ for $a = 1.55$, $\epsilon = 0.1$, and system sizes as shown in the legend. The full peak height for $N = 8192$ at $q = 1$ is 34.

Fig. 2 – Distribution of cluster sizes for the same parameters as before.

have found that in the case of one-band chaos (which appears for the individual map near $a^* = 1.56$), the binary sequence for a chaotic replica changes sign in an uncorrelated fashion with respect to a second replica (be this periodic or chaotic) and always returns an almost zero value of the overlap in the limit of long averaging times T. For two-band chaos and for periodic orbits, the overlap (2) is not vanishing and is well defined, provided the maximization with respect to phase shifts is performed for the periodic orbits. It should be noted that periodic dynamics is more typical in the clustering regime of GCLM than chaotic dynamics, which is found only inside relatively narrow regions of the parameter space. Quasiperiodic trajectories are rare and were not observed for the considered parameters.

To analyze the distribution of overlaps, their histograms were constructed. The interval $[0, 1]$ of possible overlaps q was divided into equal boxes of width 0.004 and the numbers of overlaps $q^{\alpha\beta}$ between randomly generated pairs (α, β) of replicas lying in different boxes have been counted. We performed averages over 2×10^4 replicas. As will be seen below, the statistical properties of GCLM may strongly depend on the size of the system and very large systems should therefore be considered. Systems with sizes up to $N = 8192$ have been analyzed. Since long computations are needed, so far we have calculated the histograms $P(q)$ for different system sizes only in several points in the parameter plane (a, ϵ), focusing our attention on the regions where a glass-like behaviour was previously suggested.

Figure 1 shows normalized histograms $P(q)$ computed for $a = 1.55$, $\epsilon = 0.1$, and several different system sizes. This choice of parameters corresponds to the "regular glass regime" reported by Vulpiani *et al.* [6]. We have seen that all orbits were periodic with period $p = 4$. Despite the same low periodicity, orbits with greatly different degrees of similarity can be found here (fig. 1). For $N \leq 2048$ the possible overlaps q between replicas are covering the whole interval from 0 to 1, with a depletion in the middle part. As the size N increases, the central depletion gets broader and at $N = 8192$ the distribution $P(q)$ approaches the form of two peaks, located close to $q = 0$ and $q = 1$. Thus, as the system gets larger, the orbits correponding to different cluster partitions become more similar. This transformation is accompanied by a gradual change in the statistical properties of observed cluster partitions. Figure 2 shows the corresponding histograms of distributions of relative cluster sizes N_k/N

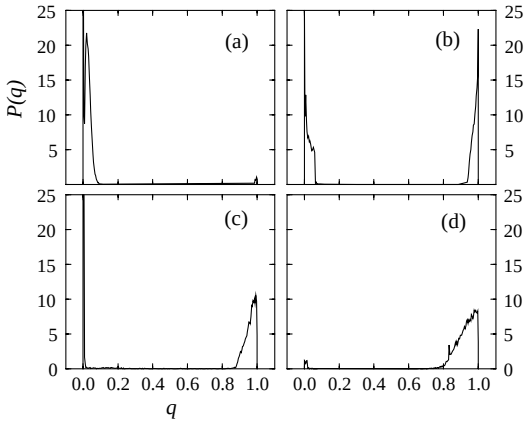

Fig. 3

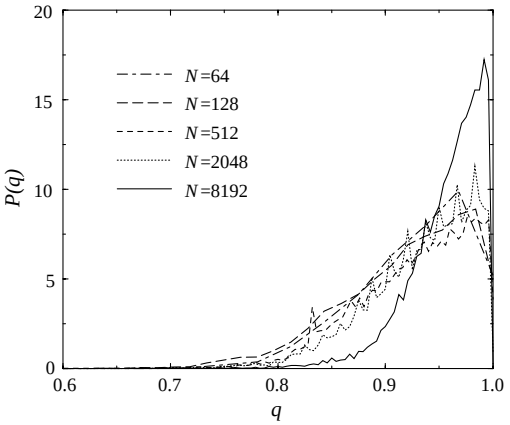

Fig. 4

Fig. 3 – Distributions $P(q)$ for $\epsilon = 0.3$, $N = 512$ and (a) $a = 1.6$, (b) $a = 1.7$, (c) $a = 1.8$, (d) $a = 1.9$.

Fig. 4 – Dependence of the overlap distribution on the system size for $a = 1.9$, $\epsilon = 0.3$, and sizes as shown in the legend.

averaged over 2×10^4 randomly generated initial conditions. For the smaller systems ($N < 512$), clusters of many different sizes can often be found, so that the cluster distribution has a broad central maximum. As N increases, the shape of the distribution is changed and two narrow sharp peaks corresponding to two different preferred cluster sizes emerge. Hence, cluster partitions generated by the system become more similar in the large-size limit.

The parameters chosen in fig. 1 lie close to the transition from dynamical clustering to the "turbulent" regime where the dynamical states of individual maps are no longer synchronized. Another interesting region of the phase diagram corresponds to the transition from dynamical clustering to the coherent regime with full global synchronization. Glassy states (*i.e.* a number of clusters of the same order as the size N of the system) have originally been reported there (see [4]). Recent studies [17, 18] show that, after very long transients, the system still approaches states with just few clusters in this parameter region. Nonetheless, the presence of such long transients indicates that the statistical properties of the system may be special here.

Figure 3 displays distributions $P(q)$ computed for a system of size $N = 512$ with coupling strength $\epsilon = 0.3$ at four values of the control parameter a. The first three points ($a = 1.6$, 1.7 and 1.8) lie inside the "glassy" region of the diagram, the last point with $a = 1.9$ is in the region of "ordered" states with few clusters and short transients. We have checked that, after sufficiently long transients, partitions with two to six clusters could be found at all these points, though the two-cluster partitions were the most frequent. The overlap distribution always consists of two peaks, close to $q = 0$ and $q = 1$. Examining individual orbits, it is found that peaks near $q = 0$ correspond now to chaotic attractors, which gradually disappear as a increases. The peak due to periodic orbits near $q = 1$ is relatively broad, so that varying degrees of similarity are observed. For example, at $a = 1.9$ the overlap can vary between 0.8 and 1, though all orbits have here the same low period $p = 2$. The dependence of the overlap distribution on the system size at $a = 1.9$ was further investigated (see fig. 4). The overlap distribution changes only slightly in the interval of sizes $64 \leq N \leq 2048$. At $N = 2048$ the distribution $P(q)$ contains weak oscillations which cannot be attributed to the lack of statistical averaging. At $N = 8192$ the small peak seen in fig. 5d near $q = 0$ disappears, and

$P(q)$ becomes stronger and narrower near $q = 1$. Again, a significant change in the statistical properties of GCLM is found as the system size is increased.

We have analyzed the hierarchical organization of replicas in GCLM. Generally, the ultrametric distance $d(A, B)$ between two elements A and B in a hierarchy is determined by the number of steps one should go up in the hierarchy to find a common ancestor of two elements A and B. If any three elements A, B and C belong to a hierarchy, the inequality $d(A, C) \leq \max\{d(A, B), d(B, C)\}$ holds. As a consequence, the two maximal distances between elements in any triad must always be equal. If overlaps $q^{\alpha\beta}$ between any two replicas α and β are uniquely determined by the ultrametric distance $d(\alpha, \beta)$ between the respective states, the overlaps between any three replicas α, β and γ must satisfy the relationship $q^{\alpha\gamma} \geq \min\{q^{\alpha\beta}, q^{\alpha\gamma}\}$, implying that the two minimal overlaps in any triad of replicas are always equal [13]. To numerically test this condition, various triads of replicas must be generated and the distribution $H(\Delta q)$ over the differences between the two minimal overlaps for any triad should be computed. If the distribution $H(\Delta q)$ is close to a delta-function at $\Delta q = 0$, the system is approximately ultrametric (see, *e.g.*, [11, 14]).

Though replica-symmetry breaking is a necessary condition for nontrivial overlap distributions, it does not yet imply exact ultrametricity. Possible deviations from strict ultrametricity have been discussed for spin glasses [13]. Recently, Parisi and Ricci-Tersenghi [20] have shown that exact ultrametricity can only hold under the conditions of "stochastic stability" (*i.e.* that each replica is in a certain sense equivalent to the others) and of "separability" (*i.e.* that all the mutual information about a pair of equilibrium configurations is already encoded in their overlap). On the other hand, if replica symmetry is not violated and overlaps between all replicas are identical, the probability distribution $H(\Delta q)$ is trivially a delta-function of Δq.

To test ultrametricity in the dynamical clustering regime of GCLM, we followed the parallel evolution of many triads of replicas α, β and γ and calculated overlaps between each pair. As the initial check, we have verified that the overlaps q determined according to eq. (2) can indeed be used to define distances between replicas. If $d(\alpha, \beta), d(\beta, \gamma)$ and $d(\alpha, \gamma)$ are the distances corresponding to a triad α, β and γ, they must always satisfy the geometrical triangle inequality $d(\alpha, \gamma) \leq d(\alpha, \beta) + d(\beta, \gamma)$. Assuming that the distance $d(\alpha, \beta)$ is a (monotonously decreasing) function of the overlap $q^{\alpha\beta}$ between replicas, this implies that the overlaps should satisfy the condition $q^{\alpha\gamma} \geq q^{\alpha\beta} + q^{\beta\gamma}$ in order that they can be meaningfully used to define the distances. We have numerically checked that the latter triangle inequality is indeed satisfied for the used overlaps with the distance $d(\alpha, \beta) = 1 - q^{\alpha\beta}$.

The numerical data was used to construct the probability distribution $H(\Delta q)$ over differences between two minimal overlaps in a triad (fig. 5 displays $H(\Delta q)$ for parameters as in fig. 1). All such distributions have a peak at $\Delta q = 0$ which grows and becomes more narrow as N increases. The shape and the size dependence of the distributions $H(\Delta q)$ in fig. 5 are strongly resembling the respective figures yielded by numerical simulations of equilibrium spin glasses at finite sizes [11, 14] and interpreted as a proof of ultrametricity in these systems. Of course, it should be remembered that, in contrast to the SK model, the overlaps in GCLM are not uniformly distributed. However, even for the largest system size $N = 8192$ the overlap distribution in fig. 1 includes both small and large overlaps, and the presence of a single narrow peak at $\Delta q = 0$ for $N = 8192$ in fig. 5 cannot be simply explained by saying that *all* overlaps are already close one to another. Figure 6 shows the functions $H(\Delta q)$ that were computed for a system of size $N = 512$ and parameters as in fig. 3. The narrow peaks at $\Delta q = 0$ are again clearly seen. This shape of the distribution is retained even at $a = 1.7$ and $a = 1.8$, when the respective overlap distributions (fig. 3b and c) have two separate peaks. Hence, we conclude that in the considered dynamical regimes the attractors of GCLM reveal some kind of hierarchical organization, though exact ultrametricity is not detected here.

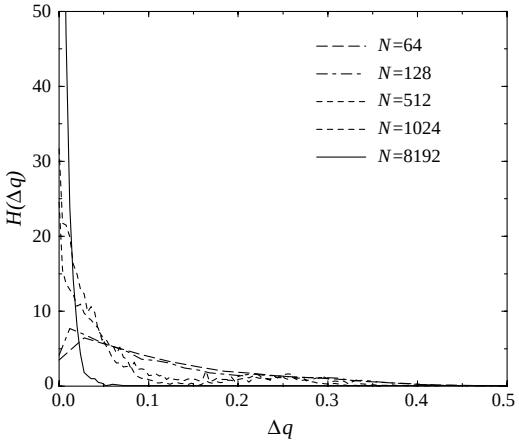

Fig. 5

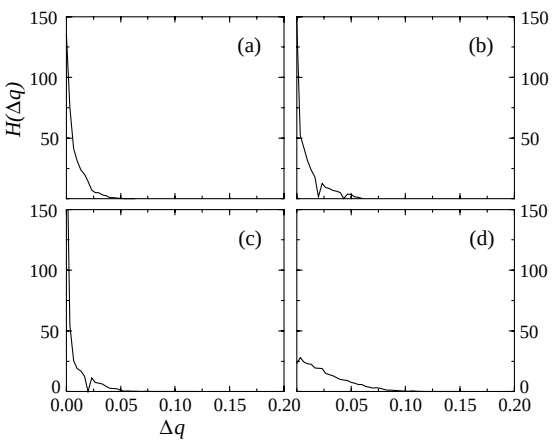

Fig. 6

Fig. 5 – Distributions $H(\Delta q)$ for systems of different sizes, other parameters as in fig. 1. The full height of the peak for $N = 8192$ at $q = 0$ is 119.

Fig. 6 – Distributions $H(\Delta q)$ for the same parameters as in fig. 3 (a-d).

The aim of the present letter was to introduce the concepts of replicas and overlap distributions for GCLM. Only the first results of numerical investigations using these notions are reported here. In our opinion, the computation of overlaps between replicas offers a new tool for the exploration of clustering in dynamical systems. We have found that in some parameter regions depending on initial conditions the system of globally coupled logistic maps can generate a great variety of orbits, characterized by mutual overlaps distributed over a wide range of values. Though an ideal hierarchical structure was not detected, our study suggests that some form of hierarchical organization is intrinsic for this system.

The results of our preliminary investigation indicate several directions for future research. Firstly, numerical simulations should be extended to systems of much larger sizes. Indeed, our simulations show that the collective behaviour of GCLM in the dynamical clustering regime undergoes a qualitative change when the size $N \approx 5000$ is reached. If the trend seen in figs. 1 and 4 is continued and the overlap distribution approaches a delta-function for the larger systems, this would mean that all replicas become statistically identical for $N \to \infty$ and thus the replica symmetry is recovered in this limit. Furthermore, the influence of noise on the glass properties of GCLM should be investigated. The introduction of noise can be important for two reasons. When equations of GCLM are iterated using a digital computer, round-off errors may lead to spurious synchronization and clustering, representing numerical artifacts. As suggested by Kaneko [21], to eliminate such undesired behaviour extremely weak noise should be added. Our previous analysis [17] has shown that, though spurious clustering can take place for chaotic attractors, it is never observed for periodic orbits which are more robust against perturbations. Since most of the distributions in this letter were constructed for parameter values where cluster partitions corresponded to different periodic orbits, we expect that they would not be affected by the introduction of weak noises. However, some results referring to the regimes with chaotic dynamics can be modified when weak noises are incorporated. The second effect, expected for relatively strong noise, is that it would smear the complex attractor structure of GCLM and restore the replica symmetry for any size of the system. Indeed, in our recent publication [22] we have seen that the dependence on initial

conditions disappears when sufficiently strong additive or multiplicative noise is applied to GCLM. The role of such strong noise would thus be similar to that of thermal fluctuations in equilibrium spin glasses. Finally, a systematic analysis of replica overlaps should be performed at many parameter points in different parts of the phase diagram of GCLM in order to obtain a full statistical description of the glass properties of this important dynamical system.

Though our present study has been performed for a particular model of GCLM, we expect that similar behaviour will be found in other large dynamical systems formed by globally coupled chaotic elements. Indeed, the collective behaviour of globally coupled Rössler oscillators [23] and ensembles of cross-coupled neural networks [24] strongly resembles that of GCLM. Recent investigations on mutual synchronization in populations of coupled chaotic electrochemical oscillators [25] provide the experimental evidence of dynamical clustering behaviour and open the possibility of an experimental test of our results.

* * *

The authors thank U. Bastolla and F. Ricci-Tersenghi for enlightening discussions and gratefully acknowledge the support of the Alexander-von-Humboldt Foundation (Germany).

REFERENCES

[1] Kaneko K., *Physica D*, **34** (1989) 1.
[2] Coullet P., Gil L. and Lega J., *Phys. Rev. Lett.*, **62** (1989) 1619.
[3] Daido H., *Phys. Rev. Lett.*, **68** (1992) 1073.
[4] Kaneko K., *Physica D*, **41** (1990) 137.
[5] Kaneko K., *J. Phys. A*, **24** (1991) 2107; *Physica D*, **124** (1998) 322.
[6] Crisanti A., Falcioni M. and Vulpiani A., *Phys. Rev. Lett.*, **76** (1996) 612.
[7] Mézard M., Parisi G. and Virasoro M. A., *Spin-Glasses Theory and Beyond* (World Scientific, Singapore) 1987.
[8] Parisi G., *J. Phys. A*, **13** (1980) 1887.
[9] Parisi G., *Phys. Rev. Lett.*, **50** (1983) 1946.
[10] Young A. P., *Phys. Rev. Lett.*, **51** (1983) 1206.
[11] Parisi G., Ritort F. and Rubí J. M., *J. Phys. A*, **24** (1991) 5307.
[12] Kisker J., Rieger H. and Schreckenberg H., *J. Phys. A*, **27** (1994) L853; Bouchaud J. P. and Mézard M., *J. Phys. I*, **4** (1994) 1109; Marinari E., Parisi G. and Ritort F., *J. Phys. A*, **27** (1994) 7647; Schmalian J. and Wolynes P. G., *Phys. Rev. Lett.*, **85** (2000) 836.
[13] Rammal R., Toulouse G. and Virasoro M. A., *Rev. Mod. Phys.*, **58** (1986) 765.
[14] Bhatt R. N. and Young A. P., *J. Magn. & Magn. Mater.*, **54-57** (1986) 191.
[15] Onuchic J. N., Wang J. and Wolynes P. G., *Chem. Phys.*, **247** (1999) 175.
[16] Park K., Rhee S. W. and Choi M. Y., *Phys. Rev. E*, **57** (1998) 5030.
[17] Manrubia S. C. and Mikhailov A. S., *Europhys. Lett.*, **50** (2000) 580
[18] Abramson G., *Europhys. Lett.*, **52** (2000) 615.
[19] A similar procedure is used in spin glasses with rotational symmetry, see Fischer K. H. and Hertz J. A., *Spin Glasses* (Cambridge University Press) 1991.
[20] Parisi G. and Ricci-Tersenghi F., *J. Phys. A*, **33** (2000) 113.
[21] Kaneko K., *Physica D*, **77** (1994) 456.
[22] Manrubia S. C. and Mikhailov A. S., *Phys. Rev. E*, **60** (1999) 157.
[23] Zanette D. H. and Mikhailov A. S., *Phys. Rev. E*, **57** (1998) 276.
[24] Zanette D. H. and Mikhailov A. S., *Phys. Rev. E*, **58** (1998) 872.
[25] Wang W., Kiss I. Z. and Hudson J. L., *Chaos*, **10** (2000) 248.